Disorder and size effects on Kondo interactions and magnetic correlations in $CePt_2$ nanocrystals

Y.Y. Chen,[1,*] P. H. Huang,[1] M.N. Ou,[1,2] C.R. Wang,[3] Y. D. Yao,[1] T. K. Lee,[1] M.Y. Ho,[1] J. M. Lawrence,[4] and C. H. Booth[5]

[1]*Institute of Physics, Academia Sinica, Taipei, Taiwan, Republic of China*
[2]*Department of Electrophysics, National Chiao Tung University , Hsinchu, Taiwan, ROC*
[3]*Department of Physics, Tunghai University, Taichung, Taiwan, Republic of China*
[4]*Department of Physics and Astronomy, University of California, Irvine, California 92697 USA*
[5]*Chemical Sciences Division, Lawrence Berkeley National Laboratory, Berkeley, California 94720 USA*

(Dated: December 13, 2006)

The evolution of the Kondo effect and magnetic correlations with size reduction in $CePt_2$ nanoparticles (3.1-26 nm) is studied by analysis of the temperature-dependent specific heat and magnetic susceptibility. The antiferromagnetic correlations diminish with size reduction. The Kondo effect predominates at small particle size with trivalent, small Kondo temperature (T_K) magnetic regions coexisting with strongly mixed valent, large T_K nonmagnetic regions. We discuss the role of structural disorder, background density of states and the electronic quantum size effect on the results.

PACS numbers: 75.30.Mb, 72.15.Qm, 75.40.Cx

It is well known that the conduction band in metals splits into discrete energy levels when the particle size is reduced to the nanoscale [1]. For a Kondo lattice system, when the mean electronic level spacing ξ becomes comparable or larger than the Kondo temperature T_K and/or the magnetic ordering temperature T_N (or T_C), the physical properties should be altered [2, 3]. The Kondo effect generated by a single magnetic impurity in nanostructures and organometallic molecules has been widely investigated in experiment and theory [2–6]. Nanostructures of Kondo lattice compounds, however, have rarely been investigated. In such materials both the Kondo effect and the Rudermann-Kittel-Kasuya-Yosida (RKKY) interaction need be taken into account [7]. Measurements of x-ray absorption fine-structure (XAFS) on $CeAl_2$ nanoparticles showed that structural disorder in the nanoparticles also plays a role in the behavior [8]. Theoretical work on Kondo lattice nanoclusters alloyed with mixed-valent impurities showed that the local Kondo temperature T_K and RKKY interactions are strongly enhanced by disorder [9]. Experimentally, the size dependence of the Kondo temperature T_K has been found to be different in different systems [7, 10, 11]. To clarify these issues and to test the extent to which the theoretical predictions [2, 3] for the Kondo impurity are valid in Kondo lattice systems, a series of specimens with systematically varied sizes should be studied.

$CePt_2$ grows in the cubic C15 ($MgCu_2$) Laves phase. It is an antiferromagnet (T_N =1.7 K) which is subject to cubic crystal field splitting between a ground state Γ_7 doublet and an excited Γ_8 quartet of trivalent cerium ions [12]. Studies [13, 14] of $CePt_{2+x}$ alloys with x=0, 0.5 and 1 show that both the strength of the magnetic correlations and the Kondo temperature decrease as the alloy parameter x increases; these effects arise primarily from site disorder (Pt on Ce sites). Here we report measurements of the specific heat C(T) and susceptibility χ(T) of a series of $CePt_2$ specimens as the particle size decreases to nanoscale.

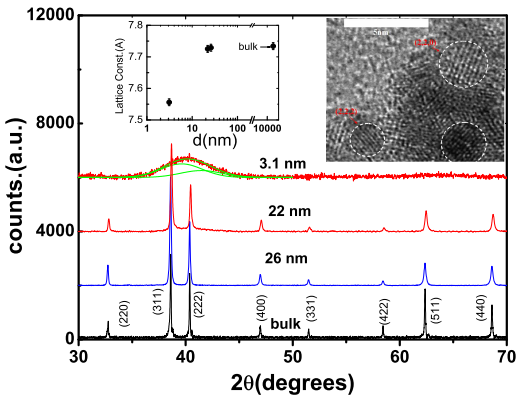

FIG. 1: X-ray diffraction patterns and Miller indices for bulk and nanoparticle $CePt_2$. Photo: HRTEM image of 3.8 nm-$CePt_2$ reveals several well-crystallized particles in which (220) and (222) planes are indicated. Inset: the lattice constant vs. diameter d.

The bulk $CePt_2$ was prepared by arc melting the constituent elements. Nanoparticles of 3.1 nm were fabricated by flash evaporation, whereas nanoparticles of d = 22 and 26 nm were grown by laser ablation. The x-ray diffraction of nanoparticles exhibited no change of structure relative to the bulk but did reveal an increase of linewidth characteristic of ultrasmall particles (Fig. 1). The lattice constants (Table 1) were determined using Rietveld refinement; the average sizes of the nanoparticles were determined by the width of the diffraction peaks

TABLE I: The physical parameters obtained by fitting C(T) and χ(T) for $CePt_2$ bulk and nanoparticles (See text for definitions)

Particle size(nm)	a_0(Å)	S_M(R ln2)or n_M	T_N(K)	n_{AF}	T_K(K)	n_K	n_K/n_M	$\Theta_D(K)$	T_{cry}(K)	C_{low} (emu/mol-K)	C_{high}	C_{high}/C(Ce3+)
Bulk	7.731	1	1.6	0.4	5.6	0.6	0.6	200	110	0.37	0.79	0.98
26±2	7.729	0.86	0.8	0.34	4.5	0.52	0.61	165	107	0.33	0.69	0.86
22±2	7.725	0.69	0.7	0.22	4.1	0.47	0.68	150	100	0.25	0.45	0.56
3.1±0.5	7.556	0.25	NA	NA	0.63	0.25	1	130	65	0.10	0.22	0.27

using the formula

$$\frac{\beta^2}{\tan^2\theta_0} = k\frac{\lambda}{L}\frac{\beta}{\tan\theta_0 \sin\theta_0} + 16e^2 \quad (1)$$

where β is the width (FWHM) of the diffraction line, θ_0 is the scattering angle, k is a constant, λ is the wavelength, L is the average particle diameter and e is the strain along (h,k,l) [15]. The lattice constant a_0 first decreases very slightly from 7.731 Å for the bulk to 7.725 Å for 22 nm ($< 0.15\%$), followed by a large $\sim 2.2\%$ decrease as d further decreases to 3.1 nm where $a_0 = 7.556$ Å (Fig. 1 inset and Table 1). The resulting particle sizes were further confirmed by high-resolution transmission electron microscopy (HRTEM) images (Fig.1 photo inset). No noticeable oxidation was detected in the nanoparticles either by x-ray diffraction or HRTEM.

The temperature dependence of the specific heat of $CePt_2$ for the bulk and nanoparticles is shown in Fig. 2. The data for bulk $CePt_2$ is in good agreement with an earlier report [13]. A sharp peak near 1.6 K is superimposed on a low-temperature bump, reflecting the coexistence of magnetic correlations and Kondo interactions. For the 26 and 22 nm samples, there is a strong decrease in the amplitude of the low temperature peak, indicating the suppression of magnetic correlations; this effect is quite similar to the effect of alloying in $CePt_{2+x}$ [13, 14]. As size is further reduced to 3.1 nm no magnetic order is seen, but instead a Kondo like upturn in the specific heat occurs below 2 K. To ascertain that the low-temperature upturn in the specific heat is of Kondo origin, further calorimetric measurements were made in external magnetic fields H=2 - 8 T (Fig. 2 inset). If the upturn were caused by an antiferromagnetic transition, an applied field would lower the ordering temperature. Instead, the anomaly actually moves up in temperature as field increases. The profile of the anomaly and its response to magnetic fields are consistent with the theoretical prediction [16] for a Kondo ion with $T_K = 0.63$K.

As discussed further below, regions of the sample with essentially trivalent "magnetic" cerium, with small Kondo temperature, coexist with regions of strongly mixed valent "nonmagnetic" cerium; the latter has a large T_K and makes a negligible contribution to the low temperature specific heat. To extract detailed information from the total low temperature specific heat C_{tot}, we need to account for the contributions C_{ph} from the lattice phonons, C_{cry} from the crystal field splitting, C_K from low-temperature Kondo interactions, and C_{AF} from the antiferromagnetic correlations. C_{ph} was determined by separate measurements on a nonmagnetic $LaPt_2$ counterpart. After phonon subtraction the crystal field T_{CF} is then estimated from the data (Fig. 3 and Table 1). We label the low temperature magnetic contribution as $C_M = C_{tot} - C_{ph} - C_{cry} = C_K + C_{AF}$. For bulk $CePt_2$, the integrated entropy $S_M = \int(C_M/T)dT$ is close to 100% of R ln2 between 0 and 15 K. This result is consistent with a Γ_7 doublet ground state with S=1/2 for trivalent cerium. Applying a similar analysis to the specific heat of the nanoparticles by taking the lattice phonon contribution from $LaPt_2$ nanoparticle counterparts, and defining the "magnetic fraction" as $n_M = S_M/R$ ln2, we find that n_M =0.86, 0.69 and 0.25 for d = 26, 22 and 3.1 nm respectively (Fig. 3). The remaining entropy (1-n_M)R ln2, presumly arising from regions of nonmagnetic, strongly mixed valent cerium with a large T_K, is transferred to higher temperature.

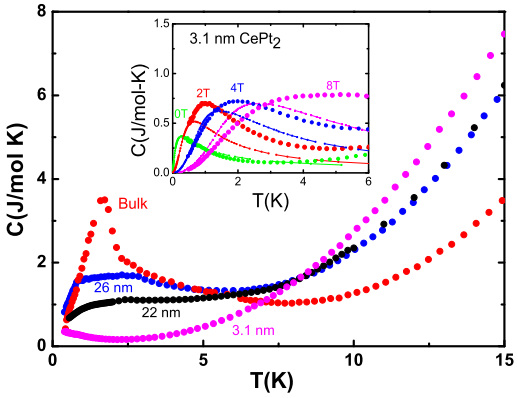

FIG. 2: C(T) versus T for bulk and nanoparticle $CePt_2$. Inset: The solid circles represent the specific heat at various magnetic fields, the lines are the theoretical calculation.

The magnetic susceptibility $1/\chi$ versus T for bulk and nanocrystalline $CePt_2$, shown in Fig. 4, confirms this decrease in the fraction of magnetic cerium. Except in the region 20-80 K where transitions begin to occur between the ground state Γ_7 doublet and the excited Γ_8 quartet [12, 13], the susceptibility can be fit to a Curie-Weiss law

χ(T) = C/(T-θ) at both high and low temperature. Here the Curie constant can be used to estimate the amount of trivalent cerium in the sample. For bulk $CePt_2$, the high temperature (low temperature) Curie constant C_h (C_l) is observed to be 0.79 (0.37) emu/K f.u.. Based on the theoretical value 0.807 emu K/f.u. for a free J=5/2 moment, the high temperature value indicates that the cerium atoms in bulk $CePt_2$ are ∼100% trivalent. This result is consistent with reports in the literature [12, 13]. The negative Weiss temperature θ_h ∼ -39 K obtained from the high-temperature region reflects demagnetization associated with the crystal-field splitting. For the nanoparticles, both C_h and C_l decrease with size reduction. The average percentages of magnetic cerium obtained from these Curie constants are ∼85%, 61% and 27% for 26, 22 and 3.1 nm respectively, in good agreement with those obtained from the specific heat measurements (Table 1).

In order to evaluate the individual contributions C_{AF} and C_K to the total magnetic specific heat C_M, we assume the contribution from magnetic correlations is negligible for T > 10 K. The preliminary Kondo contribution can then be extracted by fitting the data for T>10 K to the theoretical Kondo specific heat C_K(Theor) for one mol of S=1/2 impurity [16]. After repeated iterations, tuning the parameters T_{cry}, T_K and the fractional magnitude n_K of the Kondo contribution C_K = $n_K C_K$(Theor), we achieve a best fit. The Néel temperatures were determined from the peak in the antiferromagnetic contribution C_{AF} = C_M - C_K ; the fractional magnitude n_{AF} of the AF contribution is defined via n_{AF} = $\int(C_{AF}/T)dT/R\ \ln 2 = n_M - n_K$. For bulk $CePt_2$ we find n_K = 0. 6 with T_K = 5.6 K and n_{AF} = 0.4 (Fig. 3(a)). For 26 nm particles, n_K = 0.52 with T_K =4.5 K and n_{AF} = 0.34 with T_N =0.8 K; for 22 nm, n_K = 0.47 with T_K =4.1 K and n_{AF} = 0.22 with T_N =0.7 K. The Néel temperature and the AF fraction n_{AF} decrease to zero when d approaches to 3.1 nm (Table 1) and the specific heat data is best fit with a Kondo contribution with n_K = 0.25 and T_K=0.63 K, with no contribution from magnetic correlations (Fig. 2 inset and Fig. 3(c)). Hence, as size decreases from the bulk to 3.1 nm, the total amount n_M of magnetic cerium decreases, the relative fraction n_{AF}/n_M of the AF contribution decreases from 40% to zero, while the relative fraction n_K/n_M of the Kondo contribution increases from 60% to 100% (Table 1).

While the fraction of the sample with small Kondo temperature arises from trivalent cerium, the fraction of nonmagnetic cerium, constituting 75% of the 3.1 nm samples, must arise from strongly mixed valent cerium with a Kondo temperature sufficiently large (> 1000 K) that it makes a negligible contribution to the specific heat (C ∼ $1/T_K$) and gives rise to the large (2.3%) decrease in lattice constant relative to the bulk. Its presence can be deduced from the L_{III}-edge XANES spectra of nanocrystalline $CePt_2$ [8] where the average 4f occupation number was found to be n_f = 0.7 for 3.8 nm $CePt_2$. This value could, for example, represent 75% of the cerium being strongly mixed valent with average f occupation n_f = 0.6 and 25% being trivalent (n_f = 1). Some of the strongly mixed valent atoms occur as cerium oxide (n_f = 0.5); for example, for the 3.8 nm sample of Ref. 8, 15% of the cerium occurred as oxide. For the current sample, since there was no visible trace of oxide in the x-ray diffraction, this may be an overestimate. The spatial distribution of the different valence states is an open question. It would be consistent with standard rare earth surface science for the larger trivalent atoms to occur at the surface. However, given that the surface-to-volume ratio increases dramatically as the particle size is reduced, the concomitant increase in the mixed valent nonmagnetic fraction suggests that mixed valent cerium resides at the surface and the trivalent cerium in the core of the nanoparticle.

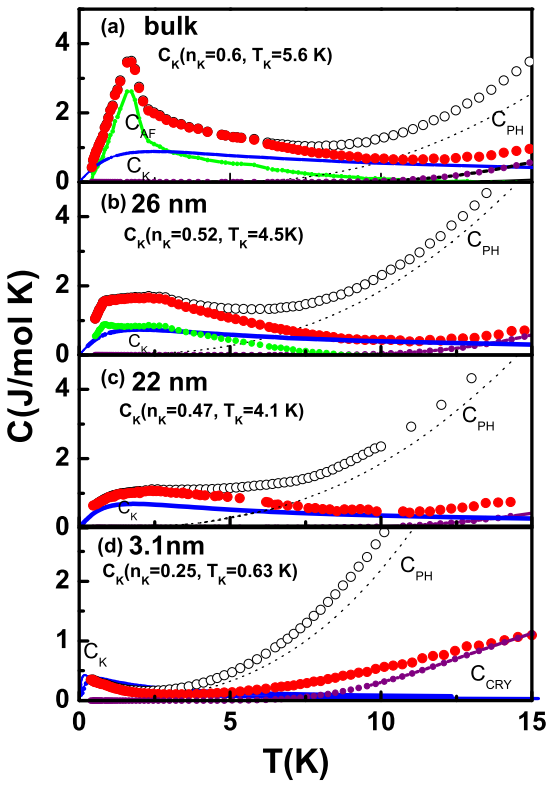

FIG. 3: The specific heat for (a) $CePt_2$ bulk (b) 26 nm (c) 22 nm (d) 3.1 nm represented by open circles. The dashed lines represent the lattice phonon contribution C_{ph}; the solid circles represent the magnetic specific heat C(T) - C_{ph}; the solid lines represent Kondo model fit C_K; and the dotted lines represent the crystal field contribution C_{cry}.

Application of Eq. 1 to our diffraction results showed that considerable lattice disorder (as represented by the strain percentage e) exists in the $CePt_2$ nanoparticles. Setting e = 0 for the bulk, we obtained e = 0.02% for d = 22 nm and e = 1.52% for d = 3.1 nm. Large bond length

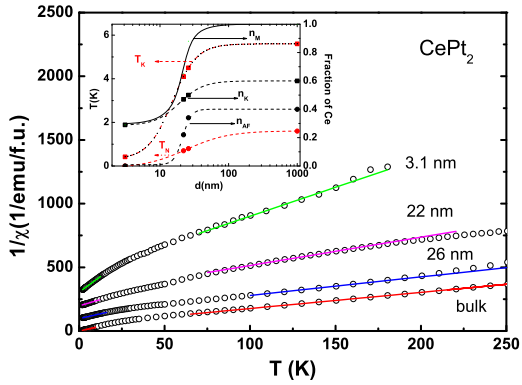

FIG. 4: The temperature dependence of the inverse susceptibility $1/\chi$ for bulk and nanoparticle $CePt_2$. The solid lines are Curie-Weiss fits. Inset: T_K and T_N (referred to the left axis) as well as the total fraction n_M of magnetic, trivalent cerium and the fraction Kondo and antiferromagnetic contributions n_K and n_{AF} (referred to the right axis) versus particle size d.

disorder was observed for $CePt_2$ and $CeAl_2$ nanocrystals through analysis of X-ray absorption fine structure (XAFS) measurements [8], where it was argued that such disorder should strongly affect the magnetic and electronic properties. In the bulk alloys $CePt_{2+x}$ (x=0-1), in which site disorder is created by extra Pt on Ce sites, the moderate decreases [14] of T_K and T_N and the fraction n_{AF} of the AF contribution as the alloy parameter x increases are very similar to those observed in the 26 and 22 nm $CePt_2$ nanoparticles, suggesting that site and/or structural disorder may be responsible for these effects observed in the larger $CePt_2$ nanocrystals.

Given the very strong mixed valence ($n_f \sim 0.6$) that we inferred above from the XANES measurement [8] for the majority (75%) of the sample at the smallest particle size (3.1 nm) the Kondo temperature of this region of the sample must be in excess of 1000 K. We note that our measurements show that the linear coefficient of specific heat γ of the nonmagnetic isostructural compound $LaPt_2$ increases from 0.005 J/mol-K^2 in the bulk to 0.010 J/mol-K^2 for 4 nm particles. This doubling of the background density of states N(0) can, when introduced into the exponential formula $T_K \sim \exp[-1/N(0)J]$, lead to a large increase in Kondo temperature and hence may explain the large increase in Kondo temperature of most of the sample.

Concerning the small Kondo temperature of the trivalent magnetic fraction of the 3.1 nm particles, it was shown in Ref. 8 that such a large reduction in T_K cannot arise from disorder. Hence the deviations plausibly can be attributed to a quantum size effect.

According to the theoretical model of Thimm et al [3] the Kondo resonance should be strongly affected when the mean conduction electron level spacing in the nanoparticle becomes larger than the Kondo temperature. According to Halperin [1], in a free-electron model the energy level spacing ξ is related to the average density of states (DOS) per spin at the Fermi surface. ξ is inversely proportional to d^3 and can be estimated from

$$\xi = \frac{(5.58nm)^3 \nu_m}{\gamma d^3} \quad (2)$$

where γ(mJ/ mol K^2) is the specific heat coefficient, and ν_m (cm^3/mol) is the molar volume. Using the values γ=5∼10 mJ/ mol K^2 for $LaPt_2$ given above, ξ is estimated to be 4.5∼9, 0.1∼0.2 and 0.06∼0.12 K for d = 3.1, 22 and 26 nm, respectively. The electronic energy level spacing $\xi \sim$ 4.5-9 K for a 3.1 nm particle is thus comparable or larger than either the Kondo temperature $T_K = 5.6$ K or the Néel temperature $T_N = 1.6$ K of bulk $CePt_2$. This lends further credence to our contention that the behaviour of the trivalent fraction of 3.1 nm particles involves a quantum size effect. We note, however, that according to the theoretical work of Ref. 2, the specific heat should be exponentially activated at low T due to the discreteness of the energy spectrum. This should lead to a low value of specific heat, rather than the rather large values actually observed, which are most clearly visible on application of a magnetic field (Fig. 2 inset).

In conclusion, we have reported the suppression of magnetic correlations and the enhancement of Kondo interactions on particle size reduction in $CePt_2$ nanoparticles. Lattice disorder is probably the origin of the variations of Kondo interactions and magnetic order for the larger nanoparticles. At the smallest particle size, 3.1. nm, an increase in the background DOS is probably responsible for the strong mixed valence in most of the sample. However, since the electronic energy level spacing ξ for the 3.1 nm particles is comparable or larger than T_K and T_N of bulk $CePt_2$, the large reduction of T_K of the trivalent fraction at ultrasmall particle size may well arise from a quantum size effect.

This work was supported by the National Council of the Republic of China under Grant No. NSC95-2120-M-001-004 and the Office of Basic Energy Sciences, U. S. Department of Energy under Contract No. AC03-76SF00098.

* cheny2@phys.sinica.edu.tw

[1] W. P. Halperin, Rev. Mod. Phys. **58**, 533 (1986).
[2] P. Schlottman, Phys. Rev. B **65**, 174407 (2002).
[3] W. B. Thimm, J. Kroha, and J. V. Delft, Phys. Rev. Lett. **82**, 2143 (1999).
[4] T. W. Odom, J.-L. Huang, C. L. Cheung, and C. M. Lieber, Science **290**, 1549 (2000).
[5] V. Madhavan, W. Chen, T. Jamneala, M. F. Crommie, and N. S. Wingreen, Science **280**, 567 (1998).
[6] C. H. Booth, M. D. Walter, M. Daniel, W. W. Lukens, and R. E. Anderson, Phys. Rev. Lett. **95**, 267202 (2005).

[7] Y. Y. Chen, Y. D. Yao, C. R. Wang, W. H. Li, C. L. Chang, T. K. Lee, T. M. Homg, J. C. Ho, and S. F. Pan, Phys. Rev. Lett. **84**, 4990 (2000).
[8] S.-W. Han, C. H. Booth, E. D. Bauer, P. H. Huang, Y. Y. Chen, and J. M. Lawrence, Phys. Rev. Lett. **97**, 097204 (2006).
[9] C. Verdozzi, Y. Luo, and N. Kioussis, Phys. Rev. B **70**, 132404 (2004).
[10] G. Bergmann, Phys. Rev. Lett. **67**, 2545 (1991).
[11] I. K. Yanson, V. V. Fisun, R. Hesper, A. V. Khotkevich, J. M. Krans, J. A. Mydosh, and J. M. van Ruitenbeek, Phys. Rev. Lett. **74**, 302 (1995).
[12] R. R. Joseph, K. A. Gschneidner, Jr., and R. F. Hungsberg, Phys. Rev. B **5**, 1878 (1972).
[13] J. M. Lawrence, Y. C. Chen, G. H. Kwei, M. F. Hundley, and J. D. Thompson, Phys. Rev. B **56**, 5 (1997).
[14] Y. Y. Chen, P. H. Huang, C. H. Booth, and J. M. Lawrence, Physica B **378-380**, 778 (2006).
[15] A. J. C. Wilson, roc. Phys. Soc. **81**, 41 (1963).
[16] P. D. Sacramenrto and P. Schlottmann, Phys. Rev. B **40**, 431 (1989).